11th Australasian Fluid Mechanics Conference
University of Tasmania, Hobart, Australia
14-18 December 1992

ENERGY REDISTRIBUTION OF NONEQUILIBRIUM HYPERVELOCITY FLOW IN A SCRAMJET DUCT

N.R. WARD and R.J. STALKER

Department of Mechanical Engineering
University of Queensland
QLD 4072, AUSTRALIA

ABSTRACT

Chemically and vibrationally frozen shock tunnel test flow is passed through a model scramjet duct with the aim of examining heat release and its effects on the flow in analogy to the heat release resulting from combustion. Experimental investigations are carried out using a differential interferometer optics system for a range of shock tunnel test conditions. The resulting images are then compared to a numerical simulation using chemical and vibrational nonequilibrium flow theory fitted to the duct shape imposed boundary conditions.

NOTATION

P = pressure
T = temperature
ρ = density
θ = flow direction
M = mach number
α = dissociation fraction
e_v = vibrational energy
γ = ratio of specific heats
δ = intake wedge angle
μ = shock angle
t = time
C_1, C_2, η_1, η_2 = chemical rate constants
C, K_2 = vibrational rate constants
θ_d = characteristic temperature for dissociation
θ_v = characteristic temperature for vibration
ρ_d = characteristic density for dissociation
e_v^* = equilibrium vibrational energy
τ = vibrational relaxation time
R = gas constant
h = enthalpy
h_q = partial derivative of h with respect to q
u = velocity
u_n = component of velocity normal to shock
a_f = frozen speed of sound
n = refractive index
I = interferogram intensity
ε = divergence angle of wollaston prism
λ = wavelength of laser light
w = displacement of wollaston prism from lens focus
f_2 = focal length of main lens
x = distance along centreline of model
W = width of model
P_s = stagnation pressure
T_s = stagnation temperature
h_s = stagnation enthalpy

INTRODUCTION

As a means of investigating the gas dynamic effects of the heat release produced by combustion of hydrogen in a scramjet duct it is intended to simulate such heat release by using chemically and vibrationally excited shock tunnel test flow to provide the energy release instead of combustion. Energy stored in the dissociation of molecules and in vibrational modes can be converted to heat energy. This evades the problems of imperfect mixing and flow disruption caused by an injector, and isolates the heat release process from the ignition process present in combustion.

The T4 shock tunnel is capable of producing high enthalpy test flow which contains significant levels of dissociation and vibrational excitation. These are frozen in the free stream flow and energy redistribution only recommences after the flow crosses the intake shocks of the scramjet, in much the same way as combustion would occur in a premixed scramjet. See figure 1.

In this paper it is aimed to investigate this heat release in a scramjet model over a range of T4 test conditions. For this study a nitrogen test gas is chosen.

Experimentally it is difficult to accurately measure flow conditions using electronic gauges without disturbing the flow. Also, such methods involving gauges only provide data at discrete locations, allowing fine detail in the flow to be missed. To avoid such problems the experimental investigations are carried out using optics to study the flow through the scramjet.

The optical system used is the *Differential Interferometer*, or *Schlieren Interferometer*. A variation on the basic system is used making it a double pass system, largely because of space constraints but also because this configuration doubles the sensitivity. See figure 2.

This system provides interferograms in which fringe shifts are related to *gradient of* refractive index within the flow field.

These experimental results obtained from the T4 shock tunnel are then compared to a numerical simulation. Chemical and vibrational non-equilibrium theory is used to computationally predict the flow pattern through the scramjet duct for the free stream conditions corresponding to the experiments.

EXPERIMENTAL METHOD

The differential interferometer used to experimentally investigate the chemically and vibrationally non-equilibrium flow in the scramjet model as produced by

the T4 shock tunnel is shown schematically in figure 2. A pulsed ruby laser is used as the light source and all mirrors are ground to an accuracy of one tenth of a wavelength or better. A spatial filter with a 5 μm pinhole is used to clean up the light source and a precision quartz wollaston prism is used with a 4 minute prism angle. The image retrieval system consists of CCD camera with 210 mm lens close mounted connected to a triggered framegrabber. Pressure gauges at the end of the shock tube trigger the camera to then trigger the laser before clearing the CCD registers and storing the image in memory of an IBM 286 computer. This is then viewed and printed.

The model used is 150 mm wide with open sides and is rear mounted in the T4 test section. Hardened gauge plate steel is used on all leading edges of the model. The intake wedges are 204 mm long and 10 degrees. The shock tunnel test section is fitted with 200 mm diameter precision crown glass windows, flat to within one tenth of a wavelength. A pitot probe is fitted above the model to check the timing of the laser against the test flow period.

NUMERICAL CALCULATIONS

The computer program predicts flow variables throughout the scramjet duct, from the free stream before the leading edge shocks to the parallel duct behind the shocks after crossing. The test model for the T4 experiments has a gap at the end of the angled intake wedges to allow the shocks to escape without reflection, and the parallel duct was designed to be narrow enough to deny entry to the expansion from the end of the wedge. This allows the definition of three 'zones' of flow, as shown in figure 3. The flow is symmetrical about the centre line, so only the bottom half is calculated.

The first zone is assumed to be chemically and vibrationally frozen, and the flow to be steady and parallel. Consequently pressure P, temperature T, density ρ, flow direction θ, mach number M, dissociation fraction α and vibrational energy e_v are all constant.

The shock angle μ for the shock emanating from the leading edge of the intake wedge, of angle δ, is calculated by solving the following equation derived by continuity considerations and the Rankine-Hugoniot equation for density ratio across a shock:

$$\frac{\tan(\delta+\mu)}{\tan\mu} = \frac{\gamma+1}{2}\left(\frac{M^2\sin^2(\delta+\mu)}{1+\frac{\gamma-1}{2}M^2\sin^2(\delta+\mu)}\right) \quad (1)$$

The flow variables are then found behind the shock using the Rankine Hugoniot equations for pressure, temperature and Mach number ratios across a shock.

As the flow passes along the surface of the wedge it adjusts chemically and vibrationally, as described by Vincenti and Kruger (1965), according to the following equations:

$$\frac{d\alpha}{dt} = [C_1 T^{\eta_1}\alpha + C_2 T^{\eta_2}(\frac{1-\alpha}{2})]\rho[(1-\alpha)e^{-\theta_d/T} - \frac{\rho}{\rho_d}\alpha^2] \quad (2)$$

and

$$\frac{de_v}{dt} = \frac{e_v^* - e_v}{\tau} \quad (3)$$

where

$$e_v^* = \frac{R\,\theta_v}{e^{\theta_v/T}-1} \quad (4)$$

$$\tau = \frac{C\,e^{(K_2/T)^{1/3}}}{P} \quad (5)$$

As it does so the temperature changes according to:

$$dT = -\frac{1}{h_T}(h_\alpha d\alpha + h_{e_v} de_v + u du) \quad (6)$$

where the enthalpy h is given by

$$h = (\frac{7}{2}+\frac{3}{2}\alpha)RT + \alpha R\theta_d + (1-\alpha)e_v \quad (7)$$

and for some q h_q is the partial derivative of $h(T,\alpha,e_v)$ with respect to q

and the component of velocity normal to the shock changes according to:

$$du_n = -\frac{u_n}{\rho h_\rho(u_n^2/a_f^2-1)}(h_\alpha d\alpha + h_{e_v} de_v) \quad (8)$$

where h_q is here the partial derivative of $h(\rho,P,\alpha,e_v)$ with respect to q

The pressure changes according to:

$$dP = -\rho u du \quad (9)$$

from conservation of momentum.

These differential equations are integrated using a second order Runge-Kuta method to obtain the chemically and vibrationally adjusting flow along the surface of the intake wedge.

As u_n changes the flow direction changes due to the component of u tangential to the shock remaining constant. At the surface of the wedge however the flow direction must be parallel to the wall. This boundary condition requires the superposition of a weak Prandtl-Meyer expansion/compression on the chemically and vibrationally adjusting flow. For a deflection of -dϕ at the wall for the adjusting flow the Prandtl-Meyer perturbation provides the equal and opposite deflection, and gives a perturbation in the other flow variables according to:

$$\frac{dP}{P} = \frac{\gamma M^2}{\sqrt{M^2-1}}d\phi \quad (10)$$

$$\frac{dM}{M} = -\frac{(1+\frac{\gamma-1}{2}M^2)}{\sqrt{M^2-1}}d\phi \quad (11)$$

$$\frac{dT}{T} = \frac{(\gamma-1)M^2}{\sqrt{M^2-1}}d\phi \quad (12)$$

These perturbations are communicated along Mach lines throughout zone 2. They are added to the adjusting flow base values which are calculated for each streamline leading off from the leading shock. In this way the flow is calculated in zone 2, and the shape of the leading shock is altered in accordance with the perturbed conditions behind it caused by the Prandtl-Meyer perturbations.

The flow in zone 3 is calculated in a similar way, using the symmetry imposed boundary condition of flow along the duct centre line being parallel to the duct centre line. For each streamline final conditions ahead of the second shock are used to calculate conditions behind the shock which are then starting conditions for the integration of the chemically and vibrationally adjusting base flow in zone 3. To these base conditions the Prandtl-Meyer perturbations are added.

From the flow variables throughout the duct the refractive index of the flow n and its gradient dn/dx can be calculated using the Gladestone-Dale equation, applied to nitrogen molecules and gas with Gladestone-Dale constants as given in Alpher and White (1958), as described by Merzkirch (1974):

$$n-1 = \rho(K_{N_2}(1-\alpha)+K_N\alpha) \qquad (13)$$

From the gradient dn/dx, a knowledge of the T4 test section and model geometries and specifications of the differential interferometer optics system the fringe intensity I of the resulting interferogram can be calculated using the equation:

$$I = \frac{1}{2}(\cos[2\pi(\frac{2\varepsilon}{\lambda})((\frac{w}{f_2})x+Wf_2(\frac{dn}{dx}))]+1) \qquad (14)$$

The numerically predicted differential interferogram is imported into the same electronics which holds the experimental interferogram. In this way a pictorial image can be produced, and this can then be compared to the experimental image.

RESULTS AND DISCUSSION

A set of experiments was carried out using the T4 shock tunnel, the results of which are presented here.

Chemical processes were initially assumed to dominate the non-equilibrium flow so the test conditions were chosen to maintain a high dissociation fraction α whilst varying the flow pressures and then to choose some other conditions with much lower α to compare. A mach five nozzle was used over this range of enthalpies and pressures. A differential interferometer image was recorded for each shot together with traces of shock speed within the shock tube, stagnation pressure at the entrance to the converging-diverging nozzle, pitot pressure at the model and the laser high voltage output trace.

The images recorded showed a curvature of the fringes after both the leading edge shock and the second shock, decaying away quite quickly in zones 2 and 3 respectively. See figure 4.

The displacement of these fringes was observed to vary for different enthalpy and pressure conditions, but in all cases the deflection of the fringes was upstream after both the first and second shocks. Fringe curvature upon entry to the heated outskirts of the boundary layer can also be clearly seen.

At the conclusion of the experiments the images were analysed and the deflection of the wollaston prism calibrated. Consequently it was confirmed that a deflection upstream signifies a raising of refractive index gradient from zero and thus increasing density. This is verified by examination of the fringe shift entering the boundary layer. This corresponds to energy *absorption* rather than heat release.

The implication of this is that despite the wide range of test conditions chosen there was not recombination in any of them.

In order to complete numerical simulations for the test conditions the free stream conditions at the entrance to the scramjet were needed. These were obtained by using a non-equilibrium nozzle flow (NENZF) program to integrate from the shock tube fill pressure, the stagnation pressure during the shot and the shock speed in the shock tube.

Numerical simulations obtained using free stream conditions found in this way predicted recombination in zone 2 at least, and an effect which was almost too small to detect when chemical rate constants as given by Vincenti and Kruger (1965) were used. It was at this stage that the previously described treatment of vibrational non-equilibrium was included, using more recent values of the vibrational rate constants as given in Sharma and Park (1990). The free stream vibrational energy used was as predicted by the method of Phinney (1964). Vibrational non-equilibrium effects were found to be highly significant to the flow.

Skinner (1992) found that at the high enthalpies at which these experiments were carried out helium contamination of the test gas from the driver gas was resulting in observations of zero dissociation of nitrogen test gas, in contradiction to the pure test gas case calculated by the NENZF program. When this was used in the numerical simulation, coupled with the more complete non-equilibrium calculation involving both vibration and chemistry, the computational results were found to be in quite good agreement with experiment. See figure 5 for the numerical simulation corresponding to figure 4. Although the fringe displacement at the start of zone 2 is not sufficient to be clearly observed for this calculation, when the calculation is carried out using a lower value of the vibrational relaxation time constant C and as a consequence a lower free stream vibrational energy, the fringe shift is clearly seen and matches experiment well. As there is an accepted high level of uncertainty in these rate constants comparison against this result is justifiable. See figure 6.

It appears that a more thorough non-equilibrium nozzle flow calculation, incorporating chemistry and vibration, and further knowledge of T4 conditions which produce helium contamination will be important in the selection of shock tunnel test conditions for future experiments. It is expected that conditions will be attainable in which the nonequilibrium flow through the scramjet model duct produces heat release rather than absorption, allowing combustion simulation, although this was not the case in the experiments covered here.

SUMMARY AND CONCLUSIONS

Experimental differential interferograms of shock tunnel test flow through a model scramjet duct have been obtained over a range of high enthalpy test conditions. In all of these cases heat absorption after the intake shocks has been observed. Helium contamination is postulated. Numerical simulations of the flow, when incorporating chemical and vibrational non-equilibrium, have been found to be in good agreement with experiment. Future experiments will involve a complete non-equilibrium nozzle flow calculation to select test conditions which produce heat release.

REFERENCES

ALPHER, R A and WHITE, D R (1958) Optical Refractivity of High Temperature Gases. I. Effects Resulting from Dissociation of Diatomic Gases. The Physics of Fluids, Volume 2 Number 2, 153-161.

MERZKIRCH, W (1974) Flow Visualisation. Academic Press, New York and London.

PHINNEY, R (1964) Nondimensional Solutions of Flows with Vibrational Relaxation. AIAA Journal, Volume 2 Number 2, 240-244.

SHARMA, S P and PARK, C (1990) Survey of simulation and diagnostic techniques for hypersonic nonequilibrium flows. J. Thermophysics. Heat Transf., Volume 4 Number 2, 129-142.

SKINNER, K (1992) Private communication. Department of Mechanical Engineering, University of Queensland, Brisbane.

VINCENTI, W G and KRUGER, C H (1965) Introduction to Physical Gas Dynamics. Robert E. Krieger Publishing Company, Malabar, Florida.

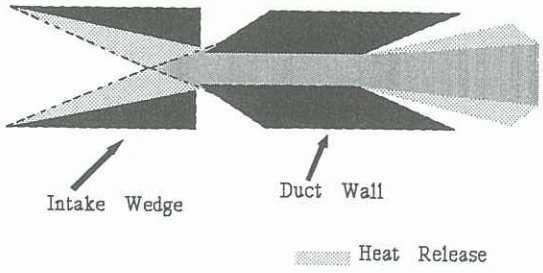

Figure 1 Heat release in a model scramjet duct.

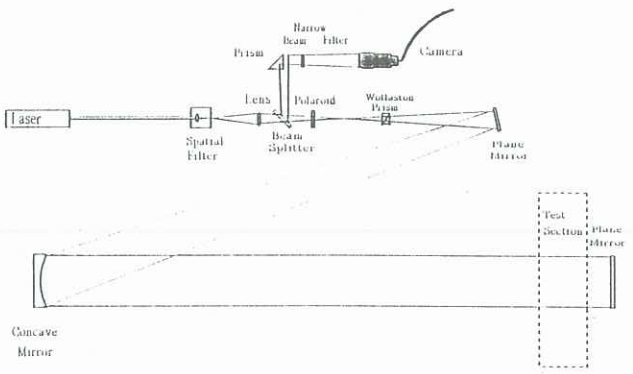

Figure 2 Differential interferometer optics system.

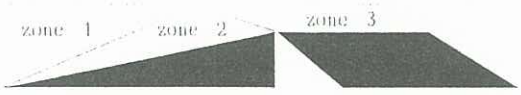

Figure 3 Geometry for numerical flow calculation.

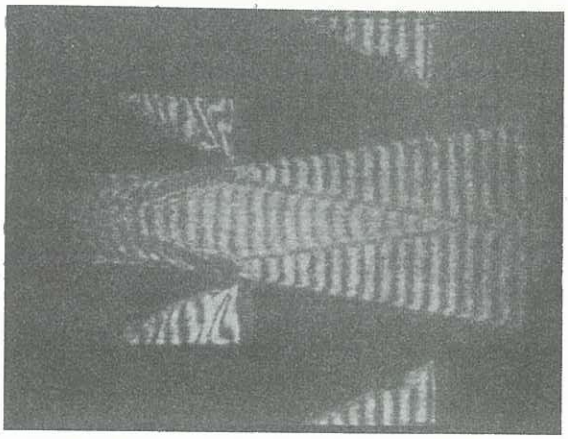

Figure 4 Experimental differential interferogram for H_s = 22 MJ/kg, P_s = 33 MPa, T_s = 9400 K.

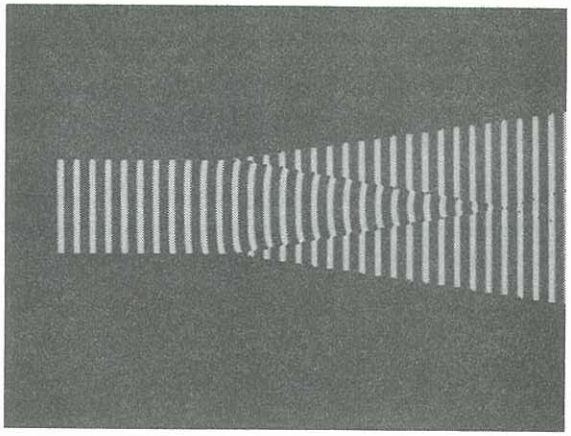

Figure 5 Numerically simulated differential interferogram for H_s = 22 MJ/kg, P_s = 33 MPa, T_s = 9400 K, frozen freestream α = 0 and e_v = 0.60 MJ/kg. Vibrational relaxation time constants used are C = 8.31×10^{-7} sec/Pa and $K_2 = 1.176 \times 10^7$ K.

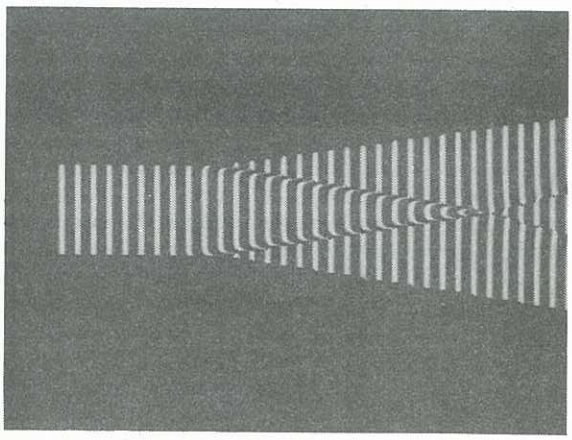

Figure 6 Numerically simulated differential interferogram for H_s = 22 MJ/kg, P_s = 33 MPa, T_s = 9400 K, frozen freestream α = 0 and e_v = 0.45 MJ/kg. Vibrational relaxation time constants used are C = 2.07×10^{-7} sec/Pa and $K_2 = 1.176 \times 10^7$ K.